

Automatic identification of schizophrenia based on EEG signals using dynamic functional connectivity analysis and 3D convolutional neural network

Mingkan Shen^{a,*}, Peng Wen^a, Bo Song^a, Yan Li^b

^a School of Engineering, University of Southern Queensland, Toowoomba, Australia

^b School of Mathematics, Physics and Computing, University of Southern Queensland, Toowoomba, Australia

ARTICLE INFO

Index terms:

ScZ
EEG
Cross mutual information
3D convolutional neural network
Default mode network

ABSTRACT

Schizophrenia (ScZ) is a devastating mental disorder of the human brain that causes a serious impact of emotional inclinations, quality of personal and social life and healthcare systems. In recent years, deep learning methods with connectivity analysis only very recently focused into fMRI data. To explore this kind of research into electroencephalogram (EEG) signal, this paper investigates the identification of ScZ EEG signals using dynamic functional connectivity analysis and deep learning methods. A time-frequency domain functional connectivity analysis through cross mutual information algorithm is proposed to extract the features in alpha band (8–12 Hz) of each subject. A 3D convolutional neural network technique was applied to classify the ScZ subjects and health control (HC) subjects. The LMSU public ScZ EEG dataset is employed to evaluate the proposed method, and a $97.74 \pm 1.15\%$ accuracy, $96.91 \pm 2.76\%$ sensitivity and $98.53 \pm 1.97\%$ specificity results were achieved in this study. In addition, we also found not only the default mode network region but also the connectivity between temporal lobe and posterior temporal lobe in both right and left side have significant difference between the ScZ and HC subjects.

1. Introduction

Schizophrenia (ScZ) is a major neuropsychiatric disorder which causes psychosis and is associated with considerable disability [1,2]. Mainly ScZ patients have persistent delusions, persistent hallucinations, disorganized thinking and highly disorganized behavior [3–5]. World Health Organization (WHO) reported that ScZ disease affects approximately 24 million people throughout the world in 2022 [6]. Electroencephalogram (EEG) as an auxiliary mean of identification, which can provide perfect performance in identification with high accuracy results between ScZ subjects and health control (HC) subjects through the scalp brain electronically signal [7]. In addition, EEG supports several benefits rather than the other medical machine application such as functional magnetic resonance imaging (fMRI) and Magnetoencephalography (MEG), which includes low-cost prize in medical machine and less reliance on trained professionals for practical application [8,9].

Complex brain networks analysis is used widely to explore brain diseases such as Alzheimer diseases, Parkinson's diseases, alcoholism, epilepsy diseases and ScZ diseases etc, [10–12]. Chen et al. proposed

function connectivity calculated through the mutual information (MI) algorithm and improved Google-net CNN models to identify the attention-deficit/hyperactivity disorder (ADHD) subjects based on EEG signal and reported a result of 94.67% accuracy [13]. They also compared the connectivity features in the support vector machine (SVM) and multilayer perceptron and received 90.16% and 92.08% accuracy, respectively. Khan et al. applied the PDC connectivity method with a 3D-CNN model to detect alcoholism EEG data, and received a result of 87.85% accuracy [12]. In our previous work, we proposed the functional connectivity through the cross mutual information (CMI) algorithm as signal processing work with a 3D-CNN method to classify the alcoholic EEG data, and received a result of $96.25 \pm 3.11\%$ accuracy [14]. Inspired by the good classification results of the method which combined the EEG brain connectivity and graph deep learning models in research, combining brain connectivity analysis and graph classification in EEG ScZ identification is proposed in this paper.

The default mode network (DMN) is a popular location for resting state brain activity analysis through the fMRI and EEG data. There are three main well-recognized area of the DMN which contains the mesial

* Corresponding author.

E-mail address: Mingkan.Shen@usq.edu.au (M. Shen).

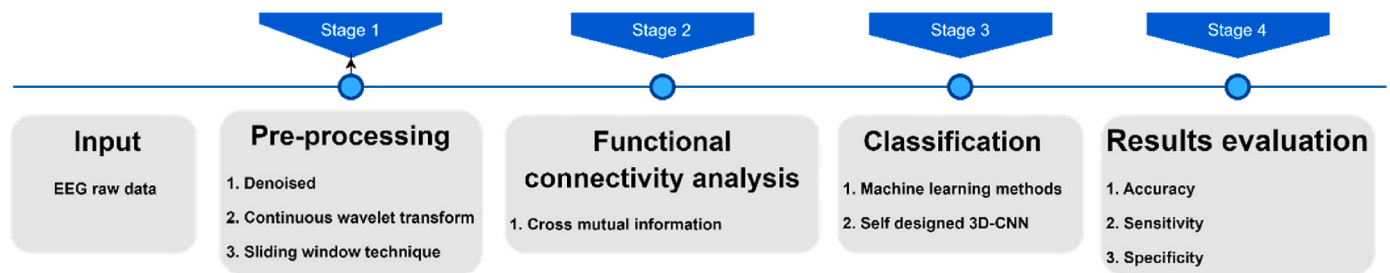


Fig. 1. The framework of automatic identification of ScZ through dynamic functional connectivity analysis and deep learning method.

prefrontal cortex (MPC), the lateral posterior cortex (LPC) and posterior cingulate cortex/precuneus (PCC) [15]. Many ScZ identification work based on fMRI data used the DMN region as the nodes through the independent component analysis [16,17]. However, Phang et al. regarded local brain network connectivity cannot fully reflect abnormal brain region communication observed in ScZ [18]. In our study, the whole brain connectivity is used to identify the ScZ and verify the effect of the DMN region through the statistical significance of connectivity.

1.1. State of art section

Many researchers have attempted to identify ScZ from EEG data through traditional signal processing method with the machine learning and deep learning models. Shoeibi et al. proposed a deep learning model which combined 1D-CNN and long short-term memories (LSTMs) to detect the ScZ EEG signal and received an accuracy percentage of 99.25% result [19]. Siuly et al. applied a Google-net based deep features with an SVM model to classify the ScZ subjects and reported a result of 98.84% accuracy, 99.02% sensitivity and 98.58% specificity [20]. They also highlighted another method through a deep residual network and SVM classifier in the same dataset and achieved 99.23% accuracy [21]. Discrete wavelet transform (DWT) and relaxed local neighbor difference pattern (RLNDip) technique with artificial neural network (ANN) is proposed by N.J. Sairamya et al. to identify the EEG ScZ signal, and they reported a maximum accuracy of 100% in their study [22]. Principal component analysis (PCA) and k-nearest neighbours (k-NN) models stated via de Miras et al. to perform ScZ patients from healthy subjects, and achieved a result of 0.87 accuracy, 0.82 sensitivity and 0.90 specificity [23].

Comparing with the traditional signal processing method used in EEG signal detection, the brain network analysis not only can achieve a satisfied detection result, but also can find the abnormal connectivity area caused by ScZ diseases. In connectivity analysis, there are mainly two methods to identification patients and HC subjects. One is using graph theory measures of complex brain network analysis to summarize the details of the brain graph and using machine learning methods to classifier the data. Kim, J.-Y et al. proposed the global and local clustering coefficient as the brain network features and received their best accuracy of 80.66% through linear discriminant analysis classifier in ScZ detection [24]. Another method is directly using the machine learning and deep learning methods to classifier the brain connectivity matrix. Panishev et al. proposed cross correlation function algorithm to construct frequency domain functional connectivity for detecting ScZ and reported results of 80% in accuracy, 76% in sensitivity and 85% specificity [25]. Zhao, Z. et al. used partial directed coherence (PDC) and phase lag index (PLI) to calculate the effective and functional connectivity matrix, and they applied the SVM model to classifier the ScZ subject and achieved 95.16% accuracy 96.15% sensitivity and 94.44% specificity results [26]. Naira, T. and C. Alberto proposed the Pearson correlation connectivity with CNN to classifier the EEG ScZ signal and reported the results 90% in accuracy, 90% in sensitivity and 90% in specificity, respectively [27]. Phang et al. developed a directed functional connectivity through PDC with vector autoregressive model, then

classified the ScZ EEG signal via a multi-domain connectome CNN model and reported a result of $91.69 \pm 4.67\%$ in accuracy, $91.11 \pm 8.31\%$ in sensitivity and $92.50 \pm 10.00\%$ in specificity [18]. Chang, Q. et al. highlighted the graph neural network (GNN) to classify ScZ connectivity features calculated by PLI and partial correlation (PC) algorithms, and reported a result of 93.33% accuracy [28].

1.2. Objectives of this study

In this study, dynamic CMI connectivity method with 3D-CNN model is proposed to identify the EEG ScZ signal. The CMI connectivity can extract the time-frequency domain features and find abnormal connectivity area caused by the ScZ diseases. In addition, the 3D-CNN models were applied and designed as a framework to classify the graph data of brain connectivity matrix. Furthermore, extension to the dynamic connectivity analysis for improving the accuracy, moving sliding window is applied in this experiment. To reduce the computational cost, the graph theory measures of complex brain network analysis is used to select the corresponding brain rhythm of ScZ identification as well. All the experiments were simulated in MATLAB 2021b software on a Dell computer with an NVIDIA 2080TI GPU.

In this paper, Section I introduced the background and brief lecture review of the study area. Section II described the EEG ScZ Dataset. The pre-processing, time-frequency brain connectivity algorithm, machine learning and deep learning classification models were summarized as well. Section III reported the results and compared the different machine learning and deep learning models of this study. In Section IV, the selection of frequency bands, statistical analysis of whole brain connectivity values and dynamic analysis were evaluated. The limitation and comparison between the proposed method with previous work were proposed in this section as well. Section V is a brief conclusion of this paper.

2. Method

There are four main steps in EEG ScZ identification, the details are described in Fig. 1. In pre-processing progress, the band-pass filter is applied to denoise the EEG raw data, and continuous wavelet transform (CWT) is stated to extract selected frequency bands data. To extend into dynamic functional connectivity, the sliding window size is selected as 30 s with 1 s overlap in this study. Then, using MI algorithm to convert the data into the functional connectivity matrix. Finally, feeding the graph matrix into the machine learning and deep learning models for the classification work.

2.1. Dataset

The publicly ScZ EEG dataset collected from Lomonosov Moscow State University (LMSU) is used to evaluate the performance through the proposed method in this study [29,30]. The dataset LMUS contains 84 subjects which includes 45 ScZ subjects and 39 HC subjects. Each subjects' data is 60-s resting eye-closed state from 16 channels (F7, F3, F4, F8, T3, C3, Cz, C4, T4, T5, P3, Pz, P4, T6, O1 and O2) with 128 Hz

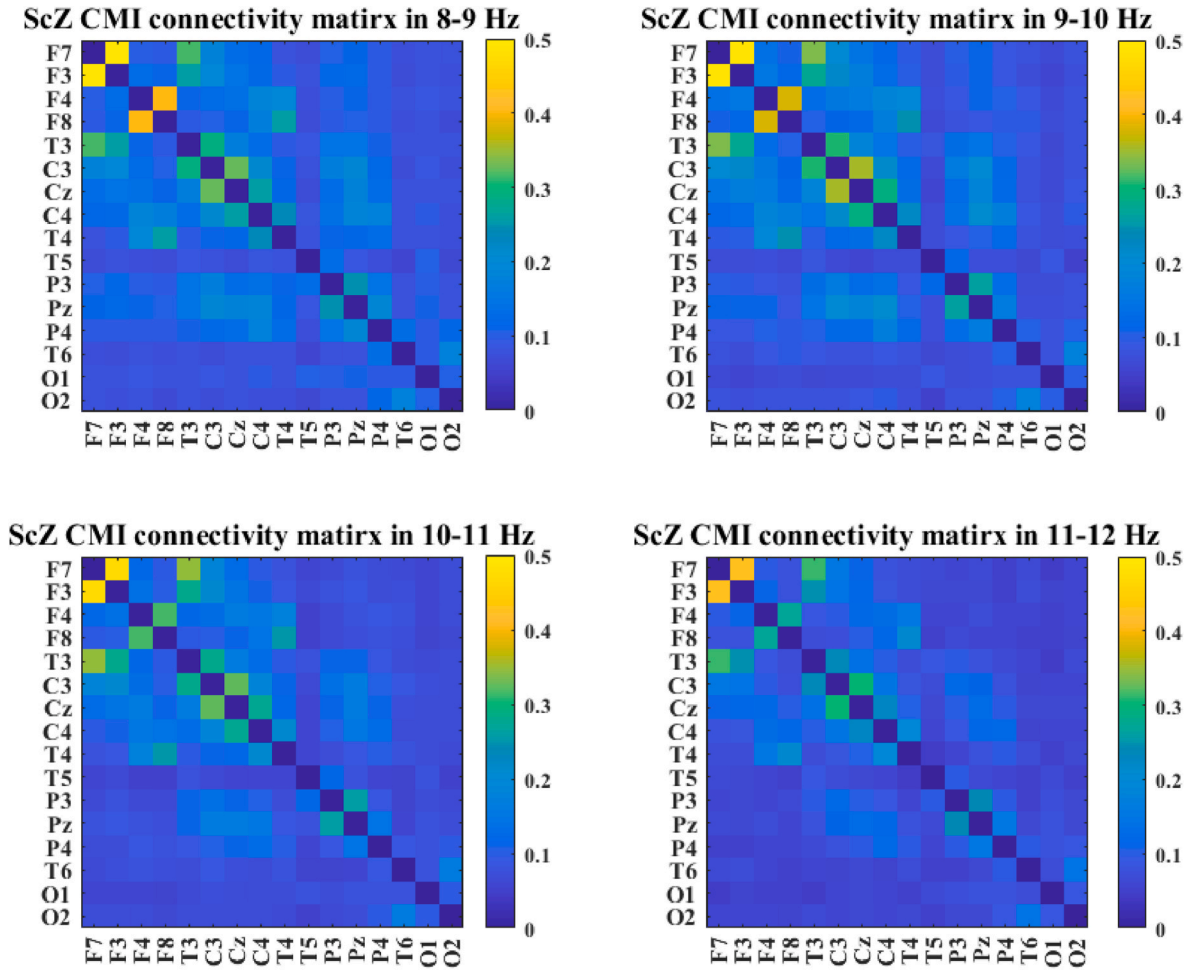


Fig. 2. CMI matrix of ScZ subject '022w1' in alpha band.

sample rate. All patients with ScZ were diagnosed at the Mental Health Research Center (MHRC) according to ScZ diagnostic criteria F20, F21, F25 of the ICD-10 classification of mental and behavioral disorders developed by the International Statistical Classification of Diseases and Related Health Problems. During the MHRC examination, the patient did not receive any chemotherapy.

2.2. Pre-processing

Sliding window technique is used in this study, to explore the dynamic changes of the functional connectivity. The sliding size was selected as 30 s within 1 s overlap. Band pass filter between 1 and 50 Hz denoised the EEG raw data through a six order Butterworth zero-phase filter algorithm.

CWT is proposed in the signal processing progress in this experiment, which converted the raw data into the time-frequency domain power spectrum in α band (8–12 Hz). The algorithm of CWT is shown in equation (1):

$$W_{x_i}(t, f) = \int x_i(\lambda) \times \overline{\varphi_{i,f}(t - \lambda)} d\lambda \quad (1)$$

where ' W_{x_i} ' is the power density, the ' f ' is the selected frequency bands, ' t ' is the time instant, and ' i ' means the number of the channel.

The mother wavelet calculated by the Morlet wavelet formula is described as follow in equation (2).

$$\varphi_{i,f}(\lambda) = A \times e^{j2\pi f(\lambda-t) \times e^{-\frac{(\lambda-t)^2}{2\sigma^2}}} \quad (2)$$

where ' σ ' is the time spread which equals to $\frac{8}{2\pi f}$.

The output of the pre-processing progress is changed into 4×3840 size of each channel data.

2.3. Cross mutual information algorithm

Based on the CWT power spectrum density, MI is used to construct the CMI functional connectivity on the time-frequency data which measures the interdependence communication between two EEG channels. The MI formula is shown in equation (3).

$$MI(F_i, F_j) = H(F_i) + H(F_j) - H(F_i, F_j) \quad (3)$$

where ' i ' is the number of the channel, the $H(F_i)$ is the entropy and the details described in equation (4).

$$H(F_i) = - \sum_{b=1}^{40} p(F_{i,b}) \log_2 p(F_{i,b}) \quad (4)$$

where F_i is the mean value of the band power. The $p(F_{i,b})$ is the probability power density.

The $H(F_i, F_j)$ is the joint entropy which describes the signal distribution, given by:

$$H(F_i, F_j) = - \sum_{b=1}^{40} p(F_{i,b}, F_{j,b}) \log_2 p(F_{i,b}, F_{j,b}) \quad (5)$$

Similarly, $p(F_{i,b}, F_{j,b})$ is the probability power density of the mean value of the band power between the channel ' i ' and ' j '. To avoid the over detrended phenomenon of $p(F_{i,b}, F_{j,b})$, the value of the bin is selected as

Table 1
The details of five group dataset.

	ScZ dataset	HC dataset
Group 1	022w1, 32w1, 33w1, 088w1, 103w, 113w1, 155w1, 156w1, 192w	S10W1, s12w1, S18W1, s20w1, S26W1, s27w1, S31W, S42W1
Group 2	219w1, 221w, 249w1, 276w1, 307w1, 312w1, 314w1, 342mw1, 382w1	s43w1, S47W1, S50W, s53w1, S55W1, S59W1, S60W, S72W1
Group 3	387-02w1, 387-03w1, 401w1, 423w, 429w1, 454-1W, 485w1, 508w1, 509w1	S78W, S85W1, s94w1, s152w1, S153W1, S154W1, S155W1, s157w1
Group 4	510-1W, 515w1, 517w1, 540w1, 548w, 573w1, 575w1, 585w1, 586w1	s158w1, S163W1, S164W1, S165W1, S167W1, S169W, s170w1, s173w1
Group 5	642w1, 683w1, 719w1, r229w1, r416w1, s083w1, S084-1W, s351w, s425w1	S174W1, s176w1, S177W1, s178w1, S179W1, S182W1, S196W1

40 in this study. In addition, the CMI formula is obtained in equation (6)

$$MI(F_i, F_j) = \sum_{b=1}^{40} p(F_{i,b}, F_{j,b}) \log_2 \frac{p(F_{i,b}, F_{j,b})}{p(F_{i,b})p(F_{j,b})} \quad (6)$$

To obtain more information from the CMI connectivity matrix, functional connectivity matrix of each Hz frequency (8–9 Hz, 9–10 Hz, 10–11 Hz, 11–12 Hz) is computed. Thus, the data of alpha band (8–12 Hz) are all converted into $16 \times 16 \times 4$ matrix through CMI algorithm. As an example, the 4-level CMI matrix of a ScZ subject ‘022w1’ of alpha band is shown in Fig. 2.

2.4. Classification via machine learning and deep learning methods

84 subjects’ data (45 ScZ subjects and 39 HC subjects) from LMSU ScZ EEG dataset was applied to evaluate the proposed method in this research. The dataset was divided into 5 groups, each group has 9 ScZ subjects and 8 HC subjects, last group have 7 HC subjects and the details are listed in Table 1. To make sure the proposed method can overcome the robustness problem, 4 groups’ data is used to training the model and another group data is used as the test data which have no overlapping of subject affiliations in the training and testing sets. In addition, the 20% random hold-out validation method is used in the training progress.

2.4.1. Three machine learning methods

Three basic machine learning methods were applied to test the ScZ EEG signal identification work which include the SVM, k-NN and decision tree (DT) methods. Because of the value of functional connectivity is symmetrical, just half data needs to feed into the machine learning models. For example, the value of F3–F4 and value of F4–F3 is same. Moreover, the CMI value of same node do not need to consider which all equals to 0. Thus, just 480 eigenvalues of 4-layer CMI connectivity matrix is used as the input.

2.4.2. Self-designed 3D-CNN model

In complex brain network analysis, researchers regarded the brain connectivity which includes structural connectivity, functional connectivity and effective connectivity (directed functional connectivity) as a graph. In this study, brain connectivity is considered as a whole graph. As the CNN has achieved good performance in photograph classification

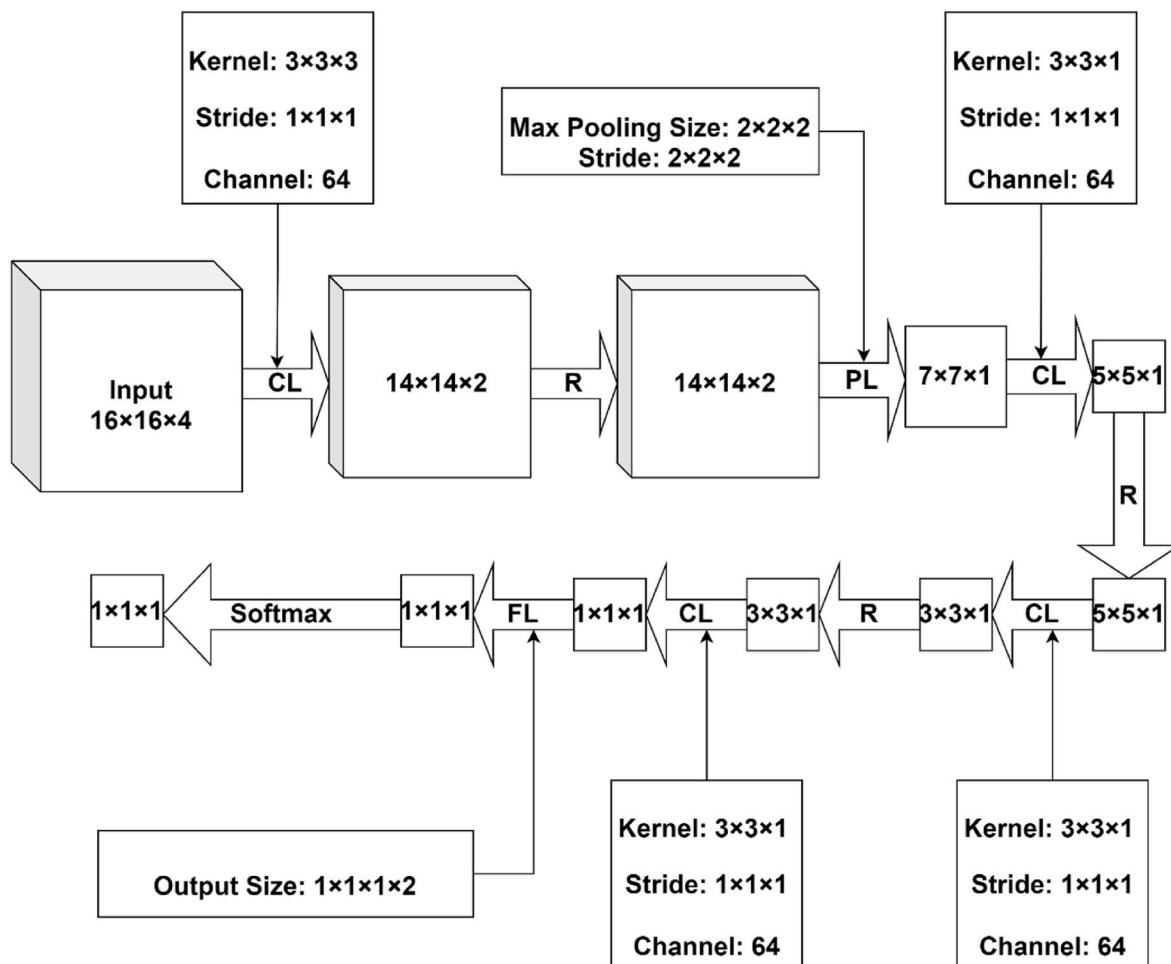


Fig. 3. Architecture of 11-layer 3D-CNN, ‘CL’ is convolution layer, ‘R’ is ReLU, ‘PL’ is max pooling layer and ‘FL’ is fully connected layer.

Table 2
The details of 3D-CNN architecture.

Layer	Input Size	Output Size	hyperparameters
3D imaged-data input	$16 \times 16 \times 4 \times 1$		
Convolution layer	$16 \times 16 \times 4 \times 1$	$14 \times 14 \times 2 \times 64$	Kernel size: $3 \times 3 \times 3$ Stride: $1 \times 1 \times 1$ Channel: 64
ReLU	$14 \times 14 \times 2 \times 64$	$14 \times 14 \times 2 \times 64$	
Max Pooling layer	$14 \times 14 \times 2 \times 64$	$7 \times 7 \times 1 \times 64$	Pooling Size: $2 \times 2 \times 2$ Stride: $2 \times 2 \times 2$
Convolution layer	$7 \times 7 \times 1 \times 64$	$5 \times 5 \times 1 \times 64$	Kernel size: $3 \times 3 \times 1$ Stride: $1 \times 1 \times 1$ Channel: 64
ReLU	$5 \times 5 \times 1 \times 64$	$5 \times 5 \times 1 \times 64$	
Convolution layer	$5 \times 5 \times 1 \times 64$	$3 \times 3 \times 1 \times 64$	Kernel size: $3 \times 3 \times 1$ Stride: $1 \times 1 \times 1$ Channel: 64
ReLU	$3 \times 3 \times 1 \times 64$	$3 \times 3 \times 1 \times 64$	
Convolution layer	$3 \times 3 \times 1 \times 64$	$1 \times 1 \times 1 \times 64$	Kernel size: $3 \times 3 \times 1$ Stride: $1 \times 1 \times 1$ Channel: 64
Fully Connected layer	$1 \times 1 \times 1 \times 64$	$1 \times 1 \times 1 \times 2$	
Softmax	$1 \times 1 \times 1 \times 2$		

work, we used 3D-CNN model to classifier the ScZ brain connectivity graph and a 10-layer 3D-CNN shown in Fig. 3 was constructed. In addition, Table 2 shows the details of the architecture.

There are four convolution layers, three ReLU layers, one max pooling layer and one fully connected layer designed in the 3D-CNN architecture. To reduce the over-fitting phenomenon, batch normalization work is added in each convolution layers. The hyperparameters of the convolution layers are selected as 64 filters, and the kernels size selected as $3 \times 3 \times 3$, $3 \times 3 \times 1$, $3 \times 3 \times 1$, and $3 \times 3 \times 1$, respectively. To improve the training speed, the max pooling layers is designed to reduce the cost of training calculation in this architectural. The hyperparameters of this max pooling layer is selected as $2 \times 2 \times 2$ size and $2 \times$

2×2 stride. ReLU is calculated follow the $f(x) = \max(0,x)$ formula. The fully connected layer which selected as the two classes classification work. Finally, a Softmax classifier for the identification using the concatenated outputs of the last layers. The training progress based on the MATLAB 2021b for testing Group 1 is shown in Fig. 4.

The 20% random hold-out validation method with 50 iterations validation frequency is used in whole comparison models include three machine learning methods and the self-designed 3D-CNN model in this study. The validation accuracy is summarized in Table 3 for the training models.

3. Results

Three parameters were calculated to evaluate the proposed method in LMSU ScZ EEG dataset include the accuracy, sensitivity, and specificity are defined as below. Accuracy is a direct parameter in method evaluation, and is defined in equation (7):

$$Acc = \frac{TP + TN}{TP + TN + FP + FN} \quad (7)$$

where ‘TP’, ‘TN’, ‘FP’, ‘FN’ correspond to the true positive, true negative, false positive and false negative.

Sensitivity is the parameter to measure the ability to recognize the patient cases correctly.

Table 3
The Validation accuracy for three machine learning methods and 3D-CNN model.

Test group	SVM	KNN	DT	3D-CNN
Validation accuracy (%)				
Group 1	100.00	100.00	96.91	98.82
Group 2	99.76	100.00	99.29	100.00
Group 3	100.00	100.00	99.06	100.00
Group 4	98.27	100.00	97.39	99.76
Group 5	99.52	100.00	98.34	100.00
Mean ±	99.51 ±	100.00 ±	98.20 ±	99.72 ±
Std	0.72	0.00	1.03	0.51

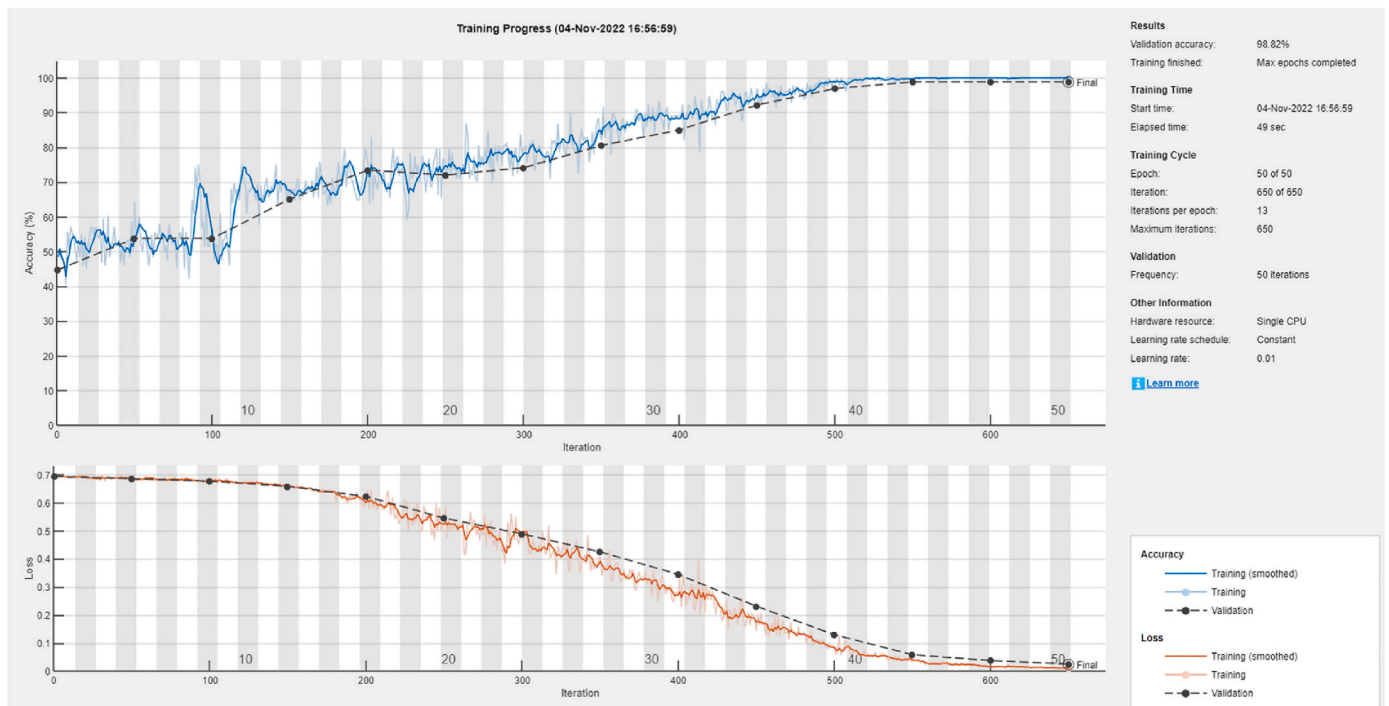


Fig. 4. The training progress for self-designed 3D-CNN model for testing Group 1.

Table 4
The test results for three machine learning methods and 3D-CNN model.

Results	Test group	SVM	k-NN	DT	3D-CNN
Accuracy (%)	Group 1	85.69	57.66	68.55	97.98
	Group 2	82.86	67.94	63.91	97.38
	Group 3	85.28	53.54	72.98	97.18
	Group 4	90.12	70.16	82.26	99.60
	Group 5	87.50	67.34	83.06	96.57
	Mean ± Std	86.29 ± 2.71	63.33 ± 7.28	74.15 ± 8.41	97.74 ± 1.15
Sensitivity (%)	Group 1	88.94	55.30	55.76	95.59
	Group 2	100.00	51.15	71.43	100.00
	Group 3	82.95	36.41	41.47	96.77
	Group 4	100.00	77.88	88.94	99.09
	Group 5	99.54	71.43	73.73	93.10
	Mean ± Std	94.29 ± 7.91	58.43 ± 16.55	66.27 ± 18.18	96.91 ± 2.76
Specificity (%)	Group 1	83.15	59.50	78.49	100.00
	Group 2	69.53	81.00	58.06	95.55
	Group 3	87.10	67.03	97.49	97.49
	Group 4	82.44	64.16	77.06	100.00
	Group 5	78.14	64.16	90.32	99.62
	Mean ± Std	80.07 ± 6.70	67.17 ± 8.19	80.28 ± 15.04	98.53 ± 1.97

$$Sen = \frac{TP}{TP + FN} \tag{8}$$

Specificity refers to the probability of a negative test, conditioned on truly being negative.

$$Spe = \frac{TN}{TN + FP} \tag{9}$$

3.1. Results for machine learning methods and 3D-CNN

SVM, k-NN, DT and 3D-CNN method are applied to detect EEG ScZ signal in this study. Comparing the results of each model, self-designed 3D-CNN model achieved the best performance which received results of 97.74 ± 1.15% accuracy, 96.91 ± 2.76% sensitivity and 98.53 ± 1.97% specificity of test data. The details are summarized in Table 4.

According to Table 4, it is obvious that the self-designed deep learning model can provide a better performance in ScZ signal identification than the SVM, k-NN and DT methods. Although these three machine learning methods can also achieve high rate in validation accuracy, they failed to provide a better classification result in the testing data. Comparing with these three machine learning methods, our self-designed 3D-CNN can overcome the robustness problem which shows the excellent identification result in the testing data of each subject. The standard deviation of our self-designed method is significant smaller than three machine learnings, it indicates that the proposed method can detect each subject in LMSU publicly ScZ dataset.

Table 5
Statistical analysis of graph theory measures in different brain rhythms.

Measures	Brain rhythms	Brain rhythms				
		δ band (1–4 Hz)	θ band (4–8 Hz)	α band (8–12 Hz)	β band (12–30 Hz)	γ band (30–60 Hz)
ScZ subjects	Modularity	5.084 ± 1.073	4.956 ± 1.015	4.632 ± 1.082	5.386 ± 1.117	6.052 ± 1.392
	Efficiency	0.205 ± 0.025	0.132 ± 0.020	0.112 ± 0.021	0.074 ± 0.017	0.064 ± 0.019
	Diffusion Efficiency	0.050 ± 0.002	0.044 ± 0.002	0.041 ± 0.003	0.033 ± 0.004	0.031 ± 0.005
	Clustering Coefficient	0.245 ± 0.027	0.162 ± 0.021	0.137 ± 0.023	0.093 ± 0.020	0.083 ± 0.022
HC subjects	Modularity	5.101 ± 0.893	4.825 ± 0.955	4.392 ± 0.766	5.428 ± 1.036	5.871 ± 1.015
	Efficiency	0.205 ± 0.020	0.131 ± 0.018	0.116 ± 0.022	0.076 ± 0.017	0.065 ± 0.017
	Diffusion Efficiency	0.050 ± 0.001	0.044 ± 0.002	0.043 ± 0.003	0.034 ± 0.004	0.031 ± 0.004
	Clustering Coefficient	0.246 ± 0.021	0.161 ± 0.020	0.139 ± 0.025	0.094 ± 0.019	0.083 ± 0.019

Table 6
The mean value of CMI values.

CMI location (Channel to Channel)	CMI values in ScZ subjects	CMI values in HC subjects
T4 - T6	0.117 ± 0.054	0.190 ± 0.090
T3 - T5	0.130 ± 0.097	0.191 ± 0.099
Cz - C4	0.193 ± 0.063	0.240 ± 0.082
Cz - Pz	0.132 ± 0.035	0.171 ± 0.100
Pz - P4	0.169 ± 0.048	0.203 ± 0.070
F3 - F4	0.149 ± 0.052	0.182 ± 0.055

4. Discussion

4.1. Brain rhythms selection through complex brain network analysis

To reduce the computational cost, selecting corresponding frequency bands is necessary. The brain network is constructed via multi-channel EEG data. Complex brain network analysis has its origins in the mathematical study of networks and is known as the graph theory [31]. The complex brain network analysis describes large-scale organization of brain networks into neurobiologically meaningful and easily computable measures [32]. Four graph theory parameters are chosen to select the brain rhythms which provide significant differences between ScZ subjects and HC subjects which include modularity, efficiency, diffusion efficiency and clustering coefficient. The statistical analysis results of the graph theory parameters in different frequency bands are listed in Table 5.

According to the statistical analysis results in four graph theory parameters, we found the alpha band (8–12 Hz) data have the most difference between the ScZ subjects and HC subjects. Thus, the alpha band is selected to analysis ScZ identification work in this study.

4.2. Statistical analysis in CMI connectivity matrix

DMN is regarded as the highly active network as compared to others which makes DMN as the key contributor in maintaining brain’s functional organization which related to the sensory, motor executive control, visual components, frontal, parietal, auditory, temporal and parietal [33]. In ScZ diseases analysis, DMN brain connectivity of fMRI data is used widely [16,17]. The DMN is identifiable in three regions which includes PCC, LPC and MPC [15]. In this experiment, the Brodmann areas (BA) is used to correspond to the DMN region [34]. Channel Pz is the precuneus location in BA07, channel Cz, F3 and F4 are the MPC part in BA08/09, BA08/09 left hemisphere and BA08/09 right hemisphere respectively [35]. The LPC region corresponds to the channel P3 and P4 which in the BA39/40 left hemisphere and BA39/40 right hemisphere area [35]. In this study, the top 6 functional connectivity with the major difference of CMI values (≥0.03) between ScZ subjects and HC subjects was shown in Table 6:

Based on statistical significance of CMI connectivity of whole brain, we found not only the DMN region but also the T4-T6 and T3-T5 connectivity have obviously difference between ScZ and HC subjects which corresponding to the area between temporal lobe and posterior temporal

Table 7

The comparison between five sliding window size.

Sliding window size	Accuracy (%)	Sensitivity (%)	Specificity (%)
2-s	80.13 ± 1.80	73.52 ± 4.99	88.14 ± 3.98
5-s	86.21 ± 3.17	79.38 ± 4.98	93.89 ± 3.44
10-s	90.27 ± 2.89	87.28 ± 6.46	93.63 ± 4.52
30-s	97.74 ± 1.15	96.91 ± 2.76	98.53 ± 1.97

Table 8

Comparison of the proposed method and previous works in EEG ScZ identification.

References	Dataset	Technique	Accuracy (%)	Sensitivity (%)	Specificity (%)
Aslan and Akin (2020) [37]	45 ScZ subjects and 39 HC subjects	STFT + VGG-16 CNN	95	95.37	94.68
Phang et al. (2020) [18]	45 ScZ subjects and 39 HC subjects	Partial directed coherence + multi-domain connectome CNN	91.69 ± 4.67	91.11 ± 8.31	89.64 ± 9.48
Shoeibi et al. (2021) [19]	14 ScZ subjects and 14 HC subjects	1D-CNN, LSTMs	99.25	–	–
Siuly et al. (2022) [20]	49 ScZ subjects and 32 HC subjects	Google-net features + SVM	98.84	99.02	98.58
Sairamya et al. (2022) [22]	45 ScZ subjects and 39 HC subjects	DWT + relaxed local neighbor difference pattern	100	–	–
de Miras et al. (2023) [23]	11 ScZ subjects and 31 HC subjects	PCA + k-NN	87	82	90
Siuly et al. (2023) [21]	49 ScZ subjects and 32 HC subjects	Deep ResNet + SVM	99.23	99.36	99.02
Proposed method	45 ScZ subjects and 39 HC subjects	CMI + 3D-CNN	97.74 ± 1.15	96.91 ± 2.76	98.53 ± 1.97

lobe in both right and left side. It is the evidence that using the whole brain connectivity analysis is essential.

4.3. Dynamic analysis with the sliding window size selection

Y. Sun et al. reported the ScZ-related aberrations in the dynamic properties of resting-state function connectivity in fMRI [36]. Considering the same issue, we use sliding window technique to extend the functional connectivity into time-varying functional connectivity. However, if the sliding window is too big, it is hard to cluster the dynamic changes in detection, and if the sliding window is too small, it will decrease the classifier accuracy. We compared the 2-s, 5-s, 10-s and 30-s sliding window sizes, and the results shows the 30-s sliding window size can achieve better performance in this study and the details summarized in Table 7.

4.4. Performance comparison with previous work and future work

Table 8 summarizes the performance of the proposed method and other peer works in EEG ScZ signal identification. The proposed method achieved a result of 97.74 ± 1.15% in accuracy, 96.91 ± 2.76% sensitivity and 98.53 ± 1.97% specificity through function connectivity analysis and 3D-CNN deep learning model. Comparing with the previous works, our proposed method can supply an excellent performance in LMSU publicly ScZ dataset (45 ScZ subjects and 39 HC subjects). Furthermore, our proposed method is capable of fuzzy localization of the ScZ disease locations as well. Through the statistical analysis in CMI connectivity matrix of whole brain network, we found the temporal lobe and posterior temporal lobe in both right and left side and the DMN region have significant differences in brain network analysis.

Comparing with SVM, k-NN and DT models, our self-designed 3D-CNN can overcome the robustness problem in classifying the CMI connectivity matrix between ScZ and HC subjects. In addition, the sliding window technique applied can capture the dynamics of ScZ signal and improve the performance of the results. However, the dynamic model depends on the sliding window technique to cluster the dynamic state more clearly. Furthermore, the source model reconstruction technique can be applied to achieve more precise localization of ScZ disease.

5. Conclusion

In this paper, the whole brain connectivity analysis is applied and implemented using mutual information algorithm. The time-frequency domain functional connectivity calculated by CWT and CMI is firstly used in ScZ identification and the frequency resolution is selected in 1 Hz in this experiment. Sliding window technique is proposed to extend the functional connectivity to time-varying functional connectivity for exploring dynamic properties of resting-state function connectivity in EEG. To reduce the computational cost, graph theory measures of complex brain network analysis is used to select brain rhythms and find alpha band (8–12 Hz) is the significance frequency band for ScZ identification work. The 3D-CNN models are applied to classify the ScZ subjects and health control subjects and achieved a result of 97.74 ± 1.15% in accuracy, 96.91 ± 2.76% sensitivity and 98.53 ± 1.97% specificity. Comparing with the machine learning methods, regarding the brain connectivity matrix as a whole graph with 3D-CNN can overcome the robustness problem. Furthermore, we analysed the CMI values in the whole connectivity and found not only the DMN region but also the connectivity between temporal lobe and posterior temporal lobe in both right and left side has significant difference between the ScZ and HC subjects.

Declaration of competing interest

The authors declare that they have no known competing financial interests or personal relationships that could have appeared to influence the work reported in this paper.

References

- [1] M.E. Shenton, et al., A review of MRI findings in schizophrenia, *Schizophrenia Res.* 49 (1–2) (2001) 1–52.
- [2] P. Krukow, et al., Abnormalities in hubs location and nodes centrality predict cognitive slowing and increased performance variability in first-episode schizophrenia patients, *Sci. Rep.* 9 (1) (2019) 1–13.
- [3] S.L. Rossell, R.A. Batty, Elucidating semantic disorganisation from a word comprehension task: do patients with schizophrenia and bipolar disorder show differential processing of nouns, verbs and adjectives? *Schizophrenia Res.* 102 (1–3) (2008) 63–68.
- [4] C. Simonsen, et al., Neurocognitive dysfunction in bipolar and schizophrenia spectrum disorders depends on history of psychosis rather than diagnostic group, *Schizophr. Bull.* 37 (1) (2011) 73–83.
- [5] J. Gomez-Pilar, et al., Altered predictive capability of the brain network EEG model in schizophrenia during cognition, *Schizophrenia Res.* 201 (2018) 120–129.
- [6] Pacific, W. and S.A.W. Hasan, Magnitude and Impact.

- [7] A. Craik, Y. He, J.L. Contreras-Vidal, Deep learning for electroencephalogram (EEG) classification tasks: a review, *J. Neural. Eng.* 16 (3) (2019), 031001.
- [8] G.G. Brown, W.K. Thompson, Functional Brain Imaging in Schizophrenia: Selected Results and Methods, *Behavioral neurobiology of schizophrenia and its treatment*, 2010, pp. 181–214.
- [9] M.-h.R. Ho, et al., Time–frequency discriminant analysis of MEG signals, *Neuroimage* 40 (1) (2008) 174–186.
- [10] P. Van Mierlo, et al., Network perspectives on epilepsy using EEG/MEG source connectivity, *Front. Neurol.* 10 (2019) 721.
- [11] H. Yu, et al., Functional brain connectivity in Alzheimer’s disease: an EEG study based on permutation disalignment index, *Phys. Stat. Mech. Appl.* 506 (2018) 1093–1103.
- [12] D.M. Khan, et al., Effective connectivity in default mode network for alcoholism diagnosis, *IEEE Trans. Neural Syst. Rehabil. Eng.* 29 (2021) 796–808.
- [13] H. Chen, Y. Song, X. Li, A deep learning framework for identifying children with ADHD using an EEG-based brain network, *Neurocomputing* 356 (2019) 83–96.
- [14] M. Shen, et al., Detection of alcoholic EEG signals based on whole brain connectivity and convolution neural networks, *Biomed. Signal Process Control* 79 (2023), 104242.
- [15] M.E. Raichle, et al., A default mode of brain function, *Proc. Natl. Acad. Sci. USA* 98 (2) (2001) 676–682.
- [16] S. Zhang, et al., Abnormal default-mode network homogeneity and its correlations with neurocognitive deficits in drug-naive first-episode adolescent-onset schizophrenia, *Schizophrenia Res.* 215 (2020) 140–147.
- [17] J. Fan, et al., Resting-state default mode network related functional connectivity is associated with sustained attention deficits in schizophrenia and obsessive-compulsive disorder, *Front. Behav. Neurosci.* 12 (2018) 319.
- [18] C.-R. Phang, et al., A multi-domain connectome convolutional neural network for identifying schizophrenia from EEG connectivity patterns, *IEEE J. Biomed. Health Inf.* 24 (5) (2019) 1333–1343.
- [19] A. Shoeibi, et al., Automatic diagnosis of schizophrenia in EEG signals using CNN-LSTM models, *Front. Neuroinf.* (2021) 58.
- [20] S. Siuly, et al., SchizoGoogLeNet: the googlenet-based deep feature extraction design for automatic detection of schizophrenia, *Comput. Intell. Neurosci.* 2022 (2022) 1–13.
- [21] S. Siuly, et al., Exploring deep residual network based features for automatic schizophrenia detection from EEG, *Phys. Eng. Sci. Med.* (2023) 1–14.
- [22] N. Sairamya, M. Subathra, S.T. George, Automatic identification of schizophrenia using EEG signals based on discrete wavelet transform and RLNDiP technique with ANN, *Expert Syst. Appl.* 192 (2022), 116230.
- [23] J.R. de Miras, et al., Schizophrenia classification using machine learning on resting state EEG signal, *Biomed. Signal Process Control* 79 (2023), 104233.
- [24] J.-Y. Kim, H.S. Lee, S.-H. Lee, EEG source network for the diagnosis of schizophrenia and the identification of subtypes based on symptom severity—a machine learning approach, *J. Clin. Med.* 9 (12) (2020) 3934.
- [25] O.Y. Panischev, et al., Use of cross-correlation analysis of EEG signals for detecting risk level for development of schizophrenia, *Biomed. Eng.* 47 (3) (2013) 153–156.
- [26] Z. Zhao, et al., Classification of schizophrenia by combination of brain effective and functional connectivity, *Front. Neurosci.* 15 (2021), 651439.
- [27] T. Naira, C. Alberto, Classification of People Who Suffer Schizophrenia and Healthy People by EEG Signals Using Deep Learning, 2020.
- [28] Q. Chang, et al., Classification of first-episode schizophrenia, chronic schizophrenia and healthy control based on brain network of mismatch negativity by graph neural network, *IEEE Trans. Neural Syst. Rehabil. Eng.* 29 (2021) 1784–1794.
- [29] N. Gorbachevskaya, S. Borisov, EEG Data of Healthy Adolescents and Adolescents with Symptoms of Schizophrenia, 2002.
- [30] S. Borisov, et al., Analysis of EEG structural synchrony in adolescents with schizophrenic disorders, *Hum. Physiol.* 31 (3) (2005) 255–261.
- [31] M. Rubinov, O. Sporns, Complex network measures of brain connectivity: uses and interpretations, *Neuroimage* 52 (3) (2010) 1059–1069.
- [32] M. Kaushal, et al., Large-scale network analysis of whole-brain resting-state functional connectivity in spinal cord injury: a comparative study, *Brain Connect.* 7 (7) (2017) 413–423.
- [33] B.A. Seitzman, et al., The state of resting state networks, *Top. Magn. Reson. Imag.: TMRI* 28 (4) (2019) 189.
- [34] D.A. Kaiser, Cortical cartography, *Biofeedback* 38 (1) (2010) 9–12.
- [35] L. Koessler, et al., Automated cortical projection of EEG sensors: anatomical correlation via the international 10–10 system, *Neuroimage* 46 (1) (2009) 64–72.
- [36] Y. Sun, et al., Dynamic reorganization of functional connectivity reveals abnormal temporal efficiency in schizophrenia, *Schizophr. Bull.* 45 (3) (2019) 659–669.
- [37] Z. Aslan, M. Akin, Automatic Detection of Schizophrenia by Applying Deep Learning over Spectrogram Images of EEG Signals, 2020.